Diagram of the States of a Grafted Polyelectrolyte Layer

O. V. Borisov,* E. B. Zhulina, and T. M. Birshtein

Institute of Macromolecular Compounds of the Russian Academy of Sciences, 199004 St. Petersburg, Russia

Received August 16, 1993; Revised Manuscript Received April 15, 1994®

ABSTRACT: An equilibrium conformational structure of a monolayer formed by polyelectrolyte chains grafted at one end onto an impermeable planar surface and immersed in a solvent is analyzed on the basis of the asymptotic solutions of the Poisson–Boltzmann equation at arbitrary grafting and charge density including the regime of nonoverlapped grafted polyions. The cases of both salf-free and salt-added solution are considered. The effect of grafted polyion orientation due to long-range interactions under the conditions of loose grafting is analyzed. The corresponding diagrams of the states of the grafted polyelectrolyte layer in the co-ordinates grafting density–charge density and grafting density–ionic strength for the cases of both good solvent and Θ-solvent are presented.

1. Introduction

The study of interfacial monolayers formed by neutral or charged macromolecules terminally attached (grafted) at the solid–liquid interface (so-called polymer brushes) is of great interest and importance in both scientific and technological aspects. Among the main technological applications of grafted polymer layers are steric stabilization of colloid dispersions, surface modification for adhesion and lubrication, and some applications in chromatography.

As shown by Alexander[1] and de Gennes,[2] in neutral polymer brushes, chains are partially stretched in the direction normal to the grafting surface due to short-range repulsive interunit interactions. This stretching takes place under conditions of both good solvent and Θ-solvent and remains even if the layer is immersed in a poor solvent.[3–6] These theoretically predicted relationships have been confirmed by low-angle neutron scattering experiments.[7–9]

The detailed intrinsic structure of polymer brushes has been studied on the basis of the SCF approach.[10–16]

The analysis of chain conformations in layers formed by polyelectrolyte (or polyampholyte) chains is expected to be very interesting and important for problems of stabilization of dispersions and in the water disperse medium by polymers, reduction of hydrodynamic friction, and other problems related to polymer behavior at water–solid interfaces because most water-soluble polymers carry ionizable groups.

As shown by Pincus and Ross[17] and by us,[18,19] the chains in polyelectrolyte brushes are also stretched in the direction normal to the grafting surface. However, in contrast to neutral brushes, this stretching is determined primarily by electrostatic interactions in the layer rather than by short-range repulsion between uncharged units. Moreover, as shown below, due to the long-range nature of the electrostatic interactions, the grafted polyelectrolyte chains become stretched in the normal direction at grafting densities below the overlapping threshold.

The main theoretical predictions concerning the dependence of the polyelectrolyte brush thickness on the chain length, grafting, and charge density were made in refs 17 and 18 for the case of a sufficiently densely grafted polyelectrolyte brush. A detailed analysis of the intrinsic structure of the polyelectrolyte brush was performed in ref 19 on the basis of the SCF approach developed previously for neutral brushes.[10–13] The analytical results obtained in ref 19 appeared to be in good agreement with earlier numerical calculations.[20,21]

The aim of the present paper is to present a general consideration of the equilibrium conformational structure of the grafted polyelectrolyte layer at an arbitrary grafting and charge density including the regime of nonoverlapped grafted polyions on the basis of the asymptotic solutions of the Poisson–Boltzmann equation. The effect of grafted polyion orientation due to long-range interactions under the conditions of sparse grafting will be analyzed. The full diagrams of the states of the grafted polyelectrolyte layer for the cases of both good solvent and Θ-solvent will be constructed. In contrast to earlier papers,[17–19] special attention will be paid to the dependence of the grafted polyion conformation on the grafting density over a wide range of its variation.

2. Model

Let us consider the layer formed by long weakly charged polyelectrolyte chains grafted at one end onto an impermeable planar surface and immersed in a dielectric solvent which is supposed to be strong (athermal) or a Θ-solvent with respect to short-range interactions between uncharged monomers. Let $N \gg 1$ be the number of monomer units in every chain, σ be the area per chain, and m be the number of uncharged monomer units between two neighboring (elementary) charged units. The total charge of each polyion is $Q = N/m$. The backbone of the polyions is supposed to be flexible (the Kuhn segment length, A, is equal to the monomer unit length, a, which, in turn, is equal to the chain thickness), and the condition of weak charging of the chains

$$m^{1/2} \gg u = l_B/a \tag{1}$$

implies that the interactions between neighboring charges do not lead to the electrostatic stiffening of the chains.[22] Here $l_B = e^2/\epsilon T$ is the Bjerrum length (e is an elementary charge, ϵ is the dielectric constant of the solvent, and T is the temperature in energy units). In water solution at normal conditions $u \cong 1$ for typical flexible polymers.

The condition of the total electroneutrality of the system results in the presence of $Q = N/m$ small mobile counterions in the solution per grafted polyion (monovalent as well as ionizable groups are presumed to be on the polyions). In principle, the solution can also contain a certain amount of small co- and counterions of added low molecular weight salt.

® Abstract published in *Advance ACS Abstracts*, June 15, 1994.

0024-9297/94/2227-4795$04.50/0

3. Salt-Free Solution

3.1. Individual Polyion. As it known, an individual polyion in salt-free solution always loses its counterions, and the interaction of charged groups on the chain has the character of unscreened Coulombic repulsion. If $Q = N/m$ is the total charge of the polyion and H is its characteristic size (end-to-end distance, for example), the stretching electrostatic force is

$$f_{el}/T = Q^2a/H^2 \tag{2}$$

(Here and below, we suppose $u \cong 1$ and omit it in all the formulas.)

The elastic force related to conformational entropy losses in the stretched chain is given by[23]

$$f_{conf}/T \cong H/Na^2, \quad \Theta\text{-solvent (Gaussian elasticity)} \tag{3.1}$$

$$f_{conf}/T \cong H^{3/2}/N^{3/2}a^{5/2}, \quad \text{good solvent} \tag{3.2}$$

The condition of force balance,

$$f_{el} \cong f_{conf} \tag{4}$$

provides[24,25]

$$H_0 \cong Nm^{-2/3}a, \quad \Theta\text{-solvent} \tag{5.1}$$

$$H_0 \cong Nm^{-4/7}a, \quad \text{good solvent} \tag{5.2}$$

(Here and below, the index "0" refers to the characteristics of an isolated polyelectrolyte chain.)

Comparison of expressions 5.1 and 5.2 with the unperturbed dimensions of Gaussian and swollen coils ($R_0 \cong N^{1/2}a$ or $N^{3/5}a$, respectively) shows that polyelectrolyte stretching, $H_0 \gg R_0$, takes place at

$$m \ll N^{3/4}, \quad \Theta\text{-solvent} \tag{6.1}$$

$$m \ll N^{7/10}, \quad \text{good solvent} \tag{6.2}$$

Introducing the notion of a "stretching blob" [26] (the part of the chain within which the chain conformation is not perturbed by an electrostatic interaction), we can envision every chain stretched by an electrostatic force to consist of a sequence of N_b blobs of size ξ

$$H \cong N_b\xi \tag{7.1}$$

$$\xi \cong T/f_{el} \tag{7.2}$$

or, taking into account eqs 2 and 5,

$$\xi_0 \cong m^{2/3}a, \quad \Theta\text{-solvent} \tag{8.1}$$

$$\xi_0 \cong m^{6/7}a, \quad \text{good solvent} \tag{8.2}$$

The chain sequence inside the blob is Gaussian under the conditions of a Θ-solvent or swollen due to excluded volume intrachain interactions in a good solvent so that the number of monomer units in every blob $g = N/N_b$ is

$$g = N/N_b \cong (\xi/a)^2, \quad \Theta\text{-solvent} \tag{9.1}$$

$$g = N/N_b \cong (\xi/a)^{5/3}, \quad \text{good solvent} \tag{9.2}$$

The dimensions of the polyions in the direction perpendicular to the end-to-end vector are given by the Gaussian law:

$$D \cong N_b^{1/2}\xi \cong N^{1/2}a, \quad \Theta\text{-solvent} \tag{10.1}$$

$$D \cong N_b^{1/2}\xi \cong N^{1/2}m^{1/7}a, \quad \text{good solvent} \tag{10.2}$$

3.2. Coulombic Interaction between Grafted Polyions. In the general case, in addition to intramolecular Coulombic repulsion, every grafted polyion experiences the mean "external" electrostatic field created by all other grafted polyions and their counterions. In contrast to an isolated polyion, the planar grafted polyelectrolyte layer retains its counterions near it even at infinite dilution (in a salt-free solution) just as an infinite charged plane.

The characteristic thickness of the counterion cloud λ is given by[27]

$$\lambda \cong l_B^{-1}\sigma/Q \tag{11}$$

Thus the distribution of counterion density and the nature of the electrostatic field in the layer are expected to depend strongly on the ratio of λ and the characteristic layer thickness, $H_\perp$.

If λ exceeds by far the characteristic layer thickness, $H_\perp$, almost all counterions leave the layer. As follows from eq 11, this regime takes place at sufficiently low surface charge densities (at large σ/Q), i.e., at low grafting density or small charge of polyions.

In this case grafted polyions and their mobile counterions form an asymmetrical double electrical layer (planar "capacitor") near the grafting surface: the charge related to the polyions is localized in the narrow ($H_\perp$) proximate region, while the counterion charge is smeared above it over a wide region ($\lambda \gg H_\perp$). As the fraction of counterions penetrating the layer and partially compensating its charge is small ($=H_\perp/\lambda \ll 1$), the surface charge per unit area in the double electrical layer is approximately equal to Q/σ. The corresponding mean electrostatic force applied to each polyion and acting in the normal direction is

$$f_{el,\perp}/T \cong Q^2a/\sigma, \quad \lambda \gg H_\perp \tag{12}$$

At sparse grafting ($\sigma \gg H_0^2$) this mean force is weak in comparison to intramolecular electrostatic repulsion (eq 2) and causes only orientation of stretched polyions (charged "sticks" of blobs) in the normal direction (Figure 1b).

It is easy to estimate the mean angle, θ, between the end-to-end vector of the polyion (the axes of the "stick" of blobs) and the direction normal to the surface from the condition

$$\Delta E_{orient} \cong f_{el,\perp}H_0(1 - \cos\theta) \cong T \tag{13}$$

where ΔE_{orient} is the increase in the electrostatic energy of the polyion due to the deviation from the most favorable direction $\theta = 0$. As follows from eq 13, the effect of polyion orientation becomes significant ($\theta \ll 1$) at $f_{el,\perp}/T \gg H_0^{-1}$ (or, taking into account eq 12, at $\sigma \ll Q^2aH_0$), and the mean value of θ in this case is given by

$$\theta \cong N_b^{-1/2}(\sigma/H_0^2)^{1/2} \tag{14}$$

Chain orientation in the normal direction results in the decrease in the lateral dimensions of the chains, which

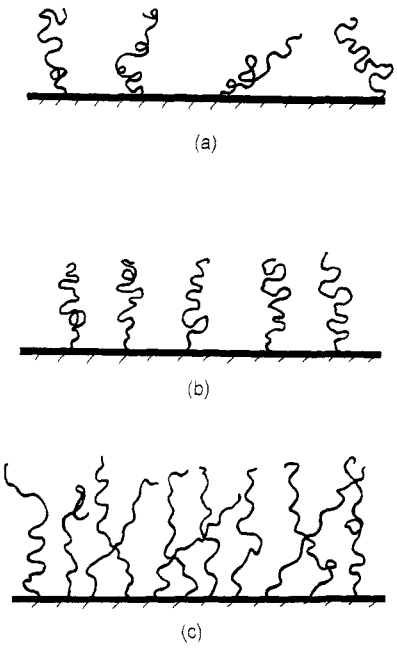

Figure 1. Grafted polyelectrolyte layer in different regimes: (a) sparse grafting, random orientation of polyions; (b) sparse grafting, strong orientation of polyions in the normal direction; (c) dense grafting (brush regime).

can be presented using eqs 7, 10, and 14 as

$$H_{\parallel}^2 = D_0^2 \cos^2\theta + H_0^2 \sin^2\theta \cong N_b\xi^2(1 + \sigma/H_0^2) \quad (15)$$

(if we suppose $\theta \ll 1$).

Hence, orientational ordering of grafted polyelectrolyte chains begins before their overlapping. The orientational order increases (θ and $H_{\parallel}$ decrease) with an increase in the grafting density (eqs 14 and 15), and at $\sigma \cong H_0^2$ (conventional condition of overlapping of neutral chains) charged chains become strongly oriented normally to the surface so that their lateral dimensions are given by the Gaussian law for the chains of blobs, $H_{\parallel} \cong N_b^{1/2}\xi \ll H_{\perp} \cong H_0$. The latter fact means that at $\sigma \cong H_0^2$ the polyions in the layer are not still really overlapped.

However, near the "overlapping" threshold, $\sigma \cong H_0^2$, the mean electrostatic force $f_{el,\perp}$ (eq 12) becomes comparable with an intramolecular force (eq 2). At higher grafting density, $\sigma \ll H_0^2$, the cooperative (intermolecular) electrostatic interactions in the grafted polyelectrolyte layer predominate over the intramolecular electrostatic interactions and determine the equilibrium structure of the layer.

If the grafting density is not very high so that the condition $\lambda \gg H_{\perp}$ is still fulfilled, the mean electrostatic force applied to every polyion and stretching it in the normal direction is given by eq 12. The balance of this stretching force and chain elasticity (eq 3)

$$f_{el,\perp} \cong f_{conf} \quad (16)$$

leads to the following expressions for the chain dimensions in the normal direction (layer thickness):

$$H_{\perp} \cong Na(Q^2a^2/\sigma), \quad \theta\text{-solvent} \quad (17.1)$$

$$H_{\perp} \cong Na(Q^2a^2/\sigma)^{2/3}, \quad \text{good solvent} \quad (17.2)$$

As follows from the "capacitor model" in this regime, the chains are stretched by a constant (independent of $H_{\perp}$) "external" force $f_{el,\perp}$ (eq 12) which is proportional to N^2. This leads to an unusual dependence of the layer thickness of the chain length ($H_{\perp} \sim N^3$ or $H_{\perp} \sim N^{7/3}$ under the conditions of θ-solvent or good solvent, respectively). In the particular case of a θ-solvent, eq 17.1 coincides with the result obtained earlier by Pincus[17] on the basis of osmotic balance arguments.

Using the concept of stretching blobs, every polyion in the layer can be represented as a sequence of blobs of size

$$\xi \cong T/f_{el,\perp} \cong \sigma/(Q^2a) \quad (18)$$

completely stretched in the normal direction, $H_{\perp} \cong N_b\xi$. Note that according to eq 18 the blob size ξ in this regime does not depend on the solvent strength. The lateral dimensions of the polyions are equal to those of the Gaussian chain of blobs:

$$H_{\parallel} \cong N_b^{1/2}\xi \cong N^{1/2}a, \quad \theta\text{-solvent} \quad (19.1)$$

$$H_{\parallel} \cong N_b^{1/2}\xi \cong N^{1/2}(\xi/a)^{1/6}a, \quad \text{good solvent} \quad (19.2)$$

As follows from eqs 12 and 17, an increase in the charge of every polyion Q and in the grafting density σ^{-1} leads to an increase in the stretching electrostatic force acting on the polyions and thus in their further stretching in the direction normal to the surface. Simultaneously, the lateral dimensions of every polyion in the layer remain constant under the conditions of θ-solvent or decrease under the conditions of strong solvent (eqs 18 and 19).

An increase in the surface charge density (increase in Q or decrease in σ) results simultaneously in an increase in the layer thickness (eq 17) and a decrease of the counterion cloud thickness λ (eq 11). When λ becomes smaller than the layer thickness $H_{\perp}$, almost all counterions are localized inside the layer, which becomes electroneutral as a whole. Moreover, the condition of total electroneutrality of the layer results in its local electroneutrality because at $\lambda \ll H_{\perp}$ the Debye screening length related to counterion density in the layer, $r_D \cong (Qa^3/\sigma H_{\perp})^{-1/2}$, is much smaller than the layer thickness: $\lambda \ll r_D \ll H_{\perp}$.

The decay of the counterion density from the mean value $Qa^3/\sigma H_{\perp}$ inside the layer to zero occurs in a narrow region $\sim r_D \ll H_{\perp}$ near the upper boundary of the layer. The fraction of counterions leaving the layer is approximately $r_D/H_{\perp} \ll 1$. As almost all counterions are retained in the volume of the layer, the stretching electrostatic force in this case should be equal to the osmotic pressure of the gas of counterions inside the layer so that

$$f_{el,\perp}/T \cong Q/H_{\perp}, \quad \lambda \ll H_{\perp} \quad (20)$$

The balance of stretching electrostatic force (eq 20) and elastic force (eq 3) determines the layer thickness in the "osmotic" regime:[17,18]

$$H_{\perp} \cong Nam^{-1/2}, \quad \theta\text{-solvent} \quad (21.1)$$

$$H_{\perp} \cong Nam^{-2/5}, \quad \text{good solvent} \quad (21.2)$$

Note that both the electrostatic stretching force (eq 20) and $H_{\perp}$ in this case do not depend on the grafting density.

In the framework of the blob picture, every chain in the layer can again be represented as completely stretched in the normal direction chain of blobs of size $\xi \cong T/f_{el,\perp}$ where the stretching force $f_{el,\perp}$ is now given by eq 20. Using eqs 20, 21, and 9, it is easy to show that in the "osmotic" regime every blob contains m monomer units and, hence, one charge, while the number of blobs, N_b, coincides with the

number $Q = N/m$ of charged groups in a chain. Thus the blob size ξ is given by

$$\xi \cong m^{1/2}a, \quad \Theta\text{-solvent} \tag{22.1}$$

$$\xi \cong m^{3/5}a, \quad \text{good solvent} \tag{22.2}$$

The lateral dimensions of polyions in the layer are described by eq 19 with $N_b = N/m$ and ξ given by eq 22.

3.3. Quasineutral Regime: Volume Interaction Dominance. Up to now, we have neglected the effect of nonelectrostatic intermolecular interactions. However, a decrease in σ or in Q can make the contributions of electrostatic and volume interchain interactions comparable. In the framework of the blob picture this corresponds to the close packing of stretching electrostatic blobs in the layer so that the boundary of the "quasineutral" regime is determined from the condition

$$\xi^2 \cong \sigma \tag{23}$$

where the size ξ of stretching blobs is given by eq 18 or 22.

At higher grafting density (or smaller polyion charge) the nonelectrostatic interactions in the layer predominant over the electrostatic interactions and determine the layer structure.

As the stretching blob size ξ in the "quasineutral" regime is also determined by volume interactions, it remains equal to $\sigma^{1/2}$ so that the layer is always represented as a system of closely packed blobs and every chain is completely stretched in the normal direction and randomly tangled in the lateral direction. Again using the relation between ξ and N_b (eq 9), we obtain the well-known results for the thickness and lateral chain dimensions in a neutral polymer brush:

$$H_\perp \cong N_b\xi \cong Na(\sigma/a^2)^{-1/2}, \quad \Theta\text{-solvent} \tag{24.1}$$

$$H_\perp \cong N_b\xi \cong Na(\sigma/a^2)^{-1/3}, \quad \text{good solvent} \tag{24.2}$$

$$H_\parallel \cong N_b{}^{1/2}\xi \cong N^{1/2}a, \quad \Theta\text{-solvent} \tag{25.1}$$

$$H_\parallel \cong N_b{}^{1/2}\xi \cong N^{1/2}(\sigma/a^2)^{1/12}a, \quad \text{good solvent} \tag{25.2}$$

3.4. Diagram of States. The diagram of states of the grafted polyelectrolyte layer in σ–m co-ordinates is presented in Figure 2.

The diagram of states contains the following regions: NC, weakly charged, sparsely grafted coils unperturbed by intra- or interchain electrostatic interactions; IS, sparsely grafted, isotropically oriented chains stretched by intramolecular electrostatic repulsion ("sticks" of stretching electrostatic blobs); OrS, sparsely grafted, orientationally ordered "sticks" of blobs; PB, polyelectrolyte brush stretched by cooperative electrostatic interactions under the condition of strong charge separation ($\lambda \gg H_\perp$); OsB, polyelectrolyte brush stretched in the "osmotic" regime ($\lambda \ll H_\perp$); NB, quasineutral regime corresponding to the predominance of nonelectrostatic volume interchain interactions.

The expressions for all structural characteristics of the layer ($H_\perp$, $H_\parallel$, ξ, and N_b) are collected in Table 1.

The boundaries of the neighboring regions of the diagram correspond to a smooth crossover of all these dependences; the equations of the boundaries are presented in Table 2.

The point (σ^*,m^*) in the diagram corresponds to the peculiar conditions of crossover of the expressions for the layer thickness $H_\perp$ (eqs 17, 21, and 24) and all other structural characteristics of the polyelectrolyte brush in all the regimes (NB, PB, and OsB). The co-ordinates of this point are $(\sigma^*,m^*)_\Theta = (N^{4/5},N^{4/5})$ in a Θ-solvent and $(\sigma^*,m^*)_+ = (N^{12/13},N^{10/13})$ in a good solvent. Note that at $\sigma \ll \sigma^*$ an increase in the polyion charge (decrease in m) leads to the transition from the quasineutral NB regime directly to the "osmotic" regime of polyelectrolyte swelling of the brush OB, while at $\sigma \gg \sigma^*$ the system passes from the NB regime to the OsB regime via the "intermediate"

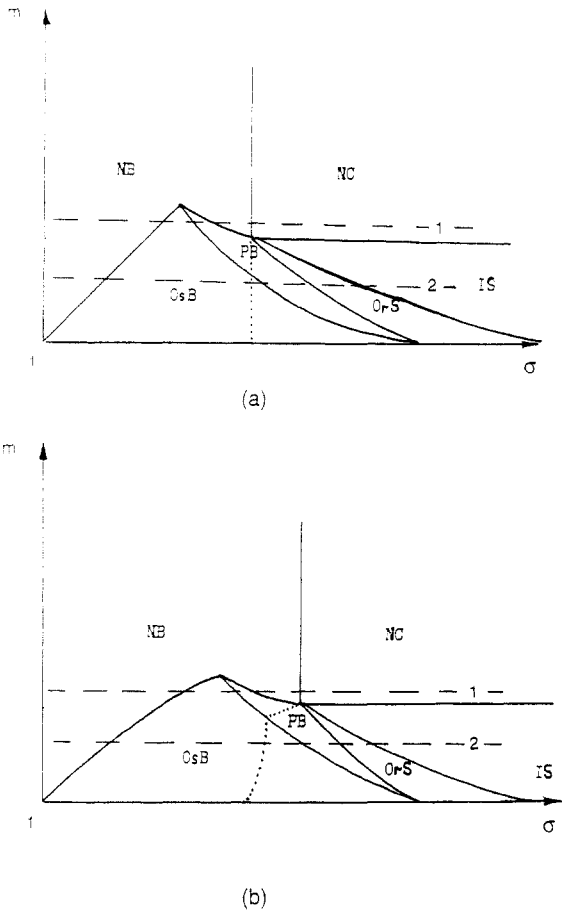

Figure 2. Diagrams of states of the grafted polyelectrolyte layer in (σ,m) co-ordinates for the cases of a Θ-solvent (a) and an athermal solvent (b); the equations of the boundaries of the regions are collected in Table 2.

Table 1. Grafted Polyelectrolyte Layer Characteristics in Different Regimes (Regions of the Diagram of States) in a Salt-Free Solution under the Conditions of Θ-Solvent and Good Solvent (a = 1)

regi	$H_\perp$	$H_\parallel$	ξ	N_b
		(a) Θ-Solvent		
NC	$N^{1/2}$	$N^{1/2}$	$N^{1/2}$	1
IS	$Nm^{-2/3}$	$\dfrac{Nm^{-2/3}}{\sigma^{1/2}N^{-1/2}m^{2/3}}$	$m^{2/3}$	$Nm^{-4/3}$
OrS				
PB	$N^3/(\sigma m^2)$	$N^{1/2}$	$m^2\sigma/N^2$	$N(N^2/(\sigma m^2))^2$
OsB	$Nm^{-1/2}$	$N^{1/2}$	$m^{1/2}$	N/m
NB	$N\sigma^{-1/2}$	$N^{1/2}$	$\sigma^{1/2}$	$N\sigma^{-1}$
		(b) Good Solvent		
NC	$N^{3/5}$	$N^{3/5}$	$N^{3/5}$	1
IS	$Nm^{-4/7}$	$\dfrac{Nm^{-4/7}}{\sigma^{1/2}N^{-1/2}m^{5/7}}$	$m^{6/7}$	$Nm^{-10/7}$
OrS				
PB	$N(N^2/(\sigma m^2))^{2/3}$	$N^{1/2}(N^2/(\sigma m^2))^{-1/6}$	$m^2\sigma/N^2$	$N(N^2/(\sigma m^2))^{5/3}$
OsB	$Nm^{-2/5}$	$N^{1/2}m^{1/10}$	$m^{3/5}$	N/m
NB	$N\sigma^{-1/3}$	$N^{1/2}\sigma^{1/12}$	$\sigma^{1/2}$	$N\sigma^{-5/6}$

Table 2. Boundaries of Regions in the Diagrams of States of the Grafted Polyelectrolyte Layer (Figure 2) under the Conditions of Θ-Solvent and Good Solvent

	NC/NB	NC/IS	IS/OrS	OrS/PB	PB/OsB	PB/NB	OsB/NB
Θ solvent	$\sigma \cong N$	$m \cong N^{3/4}$	$m \cong (N^3/\sigma)^{3/8}$	$m \cong (N^2/\sigma)^{3/4}$	$m \cong (N^2/\sigma)^{2/3}$	$m \cong N\sigma^{-1/4}$	$m \cong \sigma$
good solvent	$\sigma \cong N^{6/5}$	$m \cong N^{7/10}$	$m \cong (N^3/\sigma)^{7/8}$	$m \cong (N^2/\sigma)^{7/8}$	$m \cong (N^2/\sigma)^{5/7}$	$m \cong N\sigma^{-1/4}$	$m \cong \sigma^{5/6}$

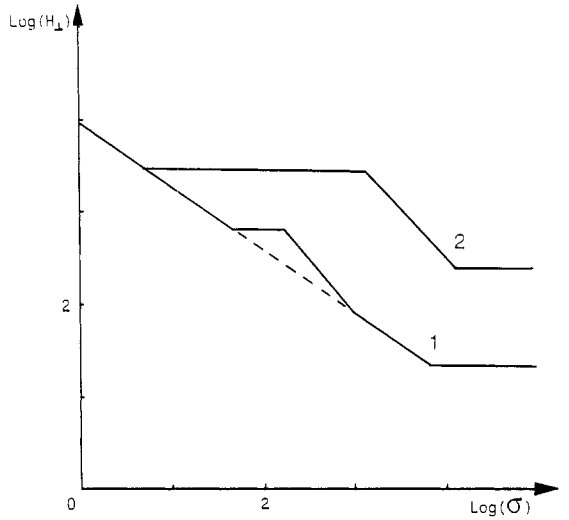

Figure 3. Schematic dependences of the layer thickness, $H_\perp$, on the grafting area per chain σ corresponding to different intersections of the diagrams in Figure 2.

PB regime. An increase in the grafting density at $m \ll m^*$ leads to the successive transition of the PB–OsB–NB (or NB–PB–OsB–NB) regimes, while at $m \gg m^*$ polyelectrolyte effects in the brush do not play any essential role at any σ.

The dashed lines in both diagrams denote the boundaries of real (geometrical) overlapping of grafted polyions in the layer, $H_\parallel^2 \cong \sigma$. We see that in the grafted polyelectrolyte layer the overlapping of neighboring chains occurs in the depth of the brush regime.

Figure 3 shows schematically the dependences of the layer thickness, $H_\perp$, on the grafting area per chain σ corresponding to different intersections of the diagram in Figure 2 (different fractions of charged units).

4. Salt-Added Solution

An addition of low molecular weight salt to the solution screens both intra- and intermolecular electrostatic interactions, thus diminishing chain stretching. Of course, the addition of salt does not affect the conformations of chains in the layer in the quasineutral regimes (NB, NC), changing only their boundaries.

4.1. Individual Polyions in a Salt-Added Solution. The conformation of an individual weakly charged polyelectrolyte molecule in the salt-added solution depends strongly on the ratio between total polyion size, salt-controlled Debye screening length $r_{Ds} \cong \varphi_s^{-1/2}a$ (where $\varphi_s a^{-3}$ is the salt concentration), and the dimensions ξ_0 of the "electrostatic" blob in a salt-free solution defined by eqs 8.1 and 8.2 (see refs 25 and 28 for a detailed discussion).

At low salt concentration, when $r_{Ds} \gg H_0$, the chain conformation is determined by unscreened intramolecular Coulombic interaction and coincides with that described in section 3.1.

At intermediate salt concentrations, when $\xi_0 \ll r_{Ds} \ll H_0$, the chain conformation at short length scales is still determined by unscreened Coulombic repulsion and every chain part within the screening length can be represented as a completely stretched sequence of blobs of size ξ_0. At length scales larger than r_{Ds}, the chain of ξ_0 blobs becomes flexible.[28] The global conformation of the polyelectrolyte molecule in this regime is determined by screened Coulombic repulsion between the parts of the chain of size r_{Ds}. This repulsion can be described as an excluded volume interaction between the rigid segments of the chain of electrostatic ξ_0 blobs: the segment thickness is equal to r_{Ds} as well as the segment length. The number of these segments in the chain is H_0/r_{Ds} so that the dimensions of the polyion as a whole are given by

$$H_0^{(s)} \cong H_0^{3/5} r_{Ds}^{2/5} \cong N^{3/5} m^{-2/5} r_{Ds}^{2/5} a^{3/5}, \quad \text{Θ-solvent} \tag{26.1}$$

$$H_0^{(s)} \cong H_0^{3/5} r_{Ds}^{2/5} \cong N^{3/5} m^{-12/35} r_{Ds}^{2/5} a^{3/5}, \quad \text{good solvent} \tag{26.2}$$

(Here and below, the index "s" denotes the salt-added case.)

Finally, at sufficiently high salt concentration, when $r_{Ds} \ll \xi_0$, the chain obeys ordinary excluded volume statistics. Under the conditions of the Θ-solvent the excluded volume parameter is determined by screened Coulombic binary interactions between the charged monomer units of the chain and is proportional to $l_B r_{Ds}^2$. Under the conditions of a good solvent (swollen ξ_0 blobs), binary repulsion between uncharged monomer units of the chain predominates over screened electrostatic repulsion between charged monomer units. Thus at $r_{Ds} \ll \xi_0$

$$H_0^{(s)} \cong N^{3/5} m^{-2/5} r_{Ds}^{2/5} a^{3/5}, \quad \text{Θ-solvent} \tag{27.1}$$

$$H_0^{(s)} \cong N^{3/5} a, \quad \text{good solvent} \tag{27.2}$$

Note that under Θ-solvent conditions the power dependences of the polyion dimensions on ξ_0 and r_{Ds} (eqs 26.1 and 27.1) coincide in the regions $\xi_0 \ll r_{Ds}$ and $r_{Ds} \ll \xi_0$, though this is not the case under good solvent conditions.

A further increase in the salt concentration (decrease in r_{Ds}) results in a decrease of "polyelectrolyte" swelling of the polyion under Θ-solvent conditions but does not affect the polyion conformation under good solvent conditions.

4.2. Salt-Controlled Brush (SB) Regimes. Let us now consider the influence of added salt on the conformations of polyelectrolyte chains under the conditions of strong interchain interactions (polyelectrolyte brush regimes).

In the absence of salt, let the layer be swollen in the OsB regime so that all counterions are contained inside the layer. Their concentration $\sim Qa^3/(\sigma H_\perp)$ determines the Debye screening length in the layer, $r_D \cong [Qa^3/(\sigma H_\perp)]^{-1/2}$.

The influence of added salt on the polyelectrolyte chain conformations in the layer becomes considerable when the salt concentration in the bulk of the solution becomes comparable to the concentration of its own counterions inside the brush, i.e., at $\varphi_s \cong Qa^3/(\sigma H_\perp)$.

When the salt concentration exceeds this value by far, the mean electrostatic force applied to grafted chains can be presented as a difference in the osmotic pressure of counterions and salt ions inside and outside the layer.[19] Under the conditions of salt dominance, this mean electrostatic force has the form

$$f_{el,\perp}^{(s)} \cong \varphi_s^{-1}Q^2/(\sigma H_\perp^2) \cong \sigma a(Qr_{Ds}/(\sigma H_\perp))^2 \quad (28)$$

Equation 28 for $f_{el,\perp}$ under conditions of salt dominance can be obtained directly from the Poisson–Boltzmann equation, but it can be clarified with the aid of the following simple arguments: the characteristic thickness of the zone with uncompensated volume charge (double electrical layer) at the upper boundary of the layer is equal to r_{Ds} and the corresponding separated charge per unit area is approximately equal to $Qr_{Ds}/(\sigma H_\perp)$ so that the stretching force per chain is given by eq 28. Note that in the salt-free "osmotic" regime the double layer thickness is approximately equal to $(Qa/(H_\perp\sigma))^{-1/2}$ and the charge per unit area is $(Qa^3/(H_\perp\sigma))^{1/2}$, which leads to eq 20 for the stretching force.

The equilibrium stretching of grafted polyions is determined by the competition between the "differential osmotic force" (eq 28) and the chain elasticity (eq 3), which provides

$$H_\perp^{(s)} \cong H^{(s)} \cong Nam^{-2/3}(r_{Ds}/a)^{2/3}(\sigma/a^2)^{-1/3}, \quad \Theta\text{-solvent} \quad (29.1)$$

$$H_\perp^{(s)} \cong H^{(s)} \cong Nam^{-4/7}(r_{Ds}/a)^{4/7}(\sigma/a^2)^{-2/7}, \quad \text{good solvent} \quad (29.2)$$

In the framework of the blob picture every chain stretched by the "differential osmotic force" can be envisioned as a completely stretched in the normal direction chain of Gaussian blobs (in Θ-solvent) or swollen blobs (in good solvent) of size

$$\xi_s \cong T/f_{el,\perp}^{(s)} \cong (\sigma r_{Ds}^{-2})(H_\perp^2/Q^2) \quad (30)$$

while the lateral chain dimensions are equal to $H_\parallel^2 \cong N_b^{(s)}\xi_s^2$.

This picture remains valid until the salt-controlled stretching blob size ξ_s is smaller than that of the electrostatic blob in salt-free solution ξ_0 or the distance between neighboring grafting points $\sigma^{1/2}$:

$$\xi_s \ll \min\{\xi_0,\sigma^{1/2}\} \quad (31)$$

At higher salt concentration inequality 31 is violated, and the size of a blob (chain sequence which retains its initial Gaussian or excluded volume statistics) is determined either by intrachain Coulombic repulsion (if $\xi_0 \ll \sigma^{1/2}$) or by interchain nonelectrostatic volume interactions (if $\xi_0 \gg \sigma^{1/2}$).

Thus, if grafting density is high enough to provide $\sigma^{1/2} \ll \xi_0$, an increase in salt concentration φ_s leads to the transition from the "salt-controlled osmotic" brush (SB) regime to the quasineutral (NB) regime; the crossover between these regimes occurs at $\xi_s \cong \sigma^{1/2}$, and at higher salt concentration any electrostatic interactions are strongly screened and do not affect chain conformation in the brush.

In the case of lower grafting density, $\sigma^{1/2} \gg \xi_0$, the picture of structural changes in the layer induced by increasing salt concentration is more complicated. As follows from eqs 2, 8, and 30, the condition $\xi_s \ll \xi_0$ (or equivalently, $H_\perp^{(s)} \gg H_0$) is fulfilled if $r_{Ds} \gg \sigma^{1/2}$, i.e., if the screening length exceeds the distance between neighboring grafting points. At higher salt concentrations, when $\xi_0 \ll r_{Ds} \ll \sigma^{1/2}$ (subregime SB′), the chain conformation on scales smaller than r_{Ds} coincides with that of an isolated polyelectrolyte chain in salt-free solution and is determined by unscreened Coulombic intrachain interactions: the chain part inside the screening length r_{Ds} can be represented as a completely stretched sequence of ξ_0 blobs. An equilibrium stretching of grafted chains on the scale of the total layer thickness is determined by screened Coulombic repulsion between chain parts of size r_{Ds}. This repulsion can be described as an excluded volume interaction between symmetrical rigid segments of size r_{Ds} of the chains of ξ_0 blobs. Corresponding equations for the brush thickness and for the lateral chain dimensions can be obtained from eqs 24.2 and 25.2 by renormalization of the segment length (a substituted by r_{Ds}) and the number of segments in the chain (N substituted by H_0/r_{Ds}) and has the following form:

$$H_\perp^{(s)} \cong H_0(\sigma/a^2)^{-1/3}(r_{Ds}/a)^{2/3} \cong Nam^{-2/3}(\sigma/a^2)^{-1/3}(r_{Ds}/a)^{2/3}, \quad \Theta\text{-solvent} \quad (32.1)$$

$$H_\perp^{(s)} \cong H_0(\sigma/a^2)^{-1/3}(r_{Ds}/a)^{2/3} \cong Nam^{-4/7}(\sigma/a^2)^{-1/3}(r_{Ds}/a)^{2/3}, \quad \text{good solvent} \quad (32.2)$$

$$H_\parallel^{(s)} \cong H_0^{1/2}(\sigma/a^2)^{1/12}(r_{Ds}/a)^{1/3}a^{1/2} \cong N^{1/2}am^{-1/3}(\sigma/a^2)^{1/12}(r_{Ds}/a)^{1/3}, \quad \Theta\text{-solvent} \quad (33.1)$$

$$H_\parallel^{(s)} \cong H_0^{1/2}(\sigma/a^2)^{1/12}(r_{Ds}/a)^{1/3}a^{1/2} \cong N^{1/2}am^{-2/7}(\sigma/a^2)^{1/12}(r_{Ds}/a)^{1/3}, \quad \text{good solvent} \quad (33.2)$$

Note that under Θ-solvent conditions eq 32.1 for the layer thickness in this subregime ($r_{Ds} \ll \sigma^{1/2}$) coincides (with the accuracy of the numerical coefficient) with eq 29.1 valid at $r_{Ds} \gg \sigma^{1/2}$. However, this is not the case under good solvent conditions (compare eqs 29.2 and 33.2).

Finally, at salt concentration high enough to provide $r_{Ds} \ll \xi_0$ the polyelectrolyte brush acquires a structure of a neutral one in a good solvent with a second virial coefficient determined either by screened electrostatic interactions between charged monomers (in a Θ-solution) or by nonelectrostatic excluded volume interactions between uncharged monomers (in a good solvent).

Under the conditions of low surface charge density, $H_\perp \ll \lambda$, the screening effect becomes significant at $r_{Ds} \ll H_\perp$ when the conditions of salt dominance in the layer already take place so that structural changes in the layer induced by an increase in the salt concentration occur as described above.

4.3. Diagram of States. Figure 4 presents a diagram of the states of a grafted polyelectrolyte layer immersed in a salt-added solution in (σ,φ_s) co-ordinates. The diagrams correspond to a sufficiently high value of polyion charge so that at $\varphi_s = 0$ the IS, OrS, PB, OsB, and NB regimes occur as the grafting density increases.

In addition to these regimes, the diagram contains regions of salt-controlled layer behavior: SC′, individual (noninteracting) grafted coils swollen due to screened Coulombic repulsion between chain parts of size r_{Ds} (on scales less than r_{Ds}, the chain can be represented as a completely stretched chain of electrostatic blobs); SC″ (in the case of Θ-solvent only), individual grafted polyelectrolyte coils swollen due to the screened Coulombic binary repulsion between chared monomers ("electrostatic excluded volume"); SB, polyelectrolyte brush stretched by the mean "differential osmotic force" ($r_{Ds} \gg \sigma^{1/2}$); SB′, polyelectrolyte brush stretched due to the screened Coulombic repulsion between chain parts of size r_{Ds} ($\xi_0 \ll r_{Ds} \ll \sigma^{1/2}$); SB″ (in the case of Θ-solvent only), polyelectrolyte brush stretched due to the screened Coulombic

Table 3. Boundaries of Regions in the Diagrams of States of the Grafted Polyelectrolyte Layer in Salt-Added Solution (Figure 4) under the Conditions of Θ-Solvent and Good Solvent

	SN/SB	SB/OsB	SB/PB	NC/SC	SC/SB	SC/IS
Θ-solvent	$\varphi_s \cong m^{-2}\sigma^{1/2}$	$\varphi_s \cong m^{-1/2}\sigma^{-1}$	$\varphi_s \cong m^4\sigma^2N^{-6}$	$\varphi_s \cong m^{-2}N^{1/2}$	$\varphi_s \cong m^{-2}\sigma^{-5/2}N^3$	$\varphi_s \cong m^{4/3}N^{-2}$
good solvent	$\varphi_s \cong m^{-2}\sigma^{1/6}$	$\varphi_s \cong m^{-3/5}\sigma^{-1}$	$\varphi_s \cong m^{8/3}\sigma^{4/3}N^{-14/3}$	$\varphi_s \cong m^{-12/7}$	$\varphi_s \cong m^{-12/7}\sigma^{-5/2}N^3$	$\varphi_s \cong m^{8/7}N^{-2}$

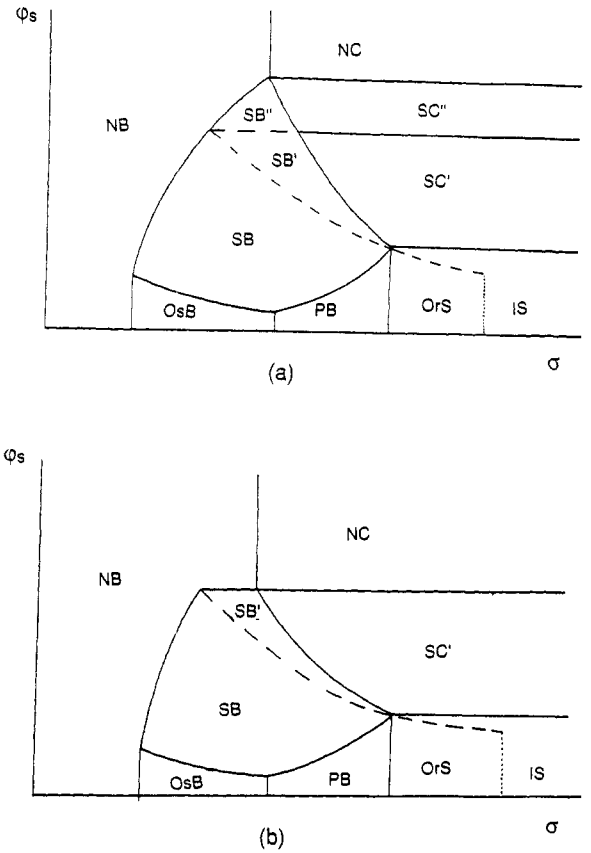

Figure 4. Diagrams of states of the grafted polyelectrolyte layer in the salt-added solution in (σ,φ_s) co-ordinates for the cases of a Θ-solvent (a) and a good solvent (b).

binary repulsion between charged monomers of different chains ("electrostatic excluded volume").

5. Conclusions

We have demonstrated that the presence of electrostatic interactions in a polymer brush considerably enriches the spectrum of different regimes of the layer behavior.

The principal difference in the behavior of the neutral and charged brushes is related to the different nature of the interactions in the system: short-range (excluded volume type) intermonomer interactions in the former case and long-range electrostatic interactions in the latter case. Whereas in neutral brushes interchain interactions are manifest at relatively high grafting densities, providing actual overlapping of neighboring chains, in charged brushes interchain interactions are seen at very sparse grafting (far from the actual overlapping threshold). This leads, in particular, to the orientational ordering of the charged polyions in the preoverlapping regime, $\sigma \gg H_0^2$. This effect is of a purely electrostatic nature and is absent in neutral brushes. The orientational ordering is well pronounced at $\sigma \gg H_0^2$ even in the case of equal dielectric constants of the solvent and that of the grafting surface, considered here. In a more realistic case when the dielectric constant of the surface is much smaller than that of the solvent, one expects the additional orientation of grafted chains due to "image charge" effects.[29]

At higher grafting densities, $\sigma \ll H_0^2$, electrostatic interactions provide stronger stretching of grafted polyions with respect to neutral chains. Only for rather dense brushes do conventional volume interactions predominate over electrostatic repulsion and determine the brush structure.

The general picture presented in this paper provides the basis for the interpretation of experimental results on polyelectrolyte brushes in a wide range of grafting densities. Unfortunately, there are no systematical experimental data on this subject at present, and only few experimental observations are available.[30-32] That is why experimental verification of the exponents in the power law dependences collected in this paper still remains an open problem.

Acknowledgment. Discussions with Prof. J.-F. Joanny were interesting and helpful. E.B.Z. and O.V.B. acknowledge the hospitality of Prof. K. Binder at Mainz University.

Appendix. Calculation of the Stretching Electrostatic Force on the Basis of the Poisson-Boltzmann Equation

In this Appendix we shall calculate the mean stretching electrostatic force acting on the grafted polyions in the "osmotic" regime in a salt-free solution and under the conditions of salt dominance on the basis of the solution of the linearized Poisson-Boltzmann equation.

Salt-Free Solution. Let the axis x be directed normally to the grafting surface which is located at $x = -H$ and the immobilized volume charge related to grafted polyions be smeared uniformly in the range of $-H \le x \le 0$ with a constant density $\rho_{im} = eQ/(\sigma H)$.

We suppose the condition $\lambda \ll H$ (where λ is still determined by eq 11) to be fulfilled so that almost all counterions are contained in the layer and the corresponding Debye screening length $r_D \ll H$. The mean concentration on counterions in the layer is

$$\bar{n} \cong -\rho_{im}/q$$

where q is the charge of a counterion and the Debye screening length is defined as

$$r_D = \kappa^{-1} = [4\pi\bar{n}q^2/(\epsilon T)]^{-1/2} \qquad \text{(A1)}$$

The Poisson equations for the mean electrostatic potential $\psi(x)$ created by immobilized charge and mobile counterions has the following form:

$$d^2\psi(x)/dx^2 = -4\pi\rho(x)/\epsilon \qquad \text{(A2)}$$

where the total charge density $\rho(x)$ is given by

$$\rho(x) = \rho_{im} + qn(x), \quad -H \le x \le 0 \qquad \text{(A3.1)}$$

$$\rho(x) = qn(x), \quad x \ge 0 \qquad \text{(A3.2)}$$

and the counterion concentration $n(x)$ is related to $\psi(x)$ by the Boltzmann equation:

$$n(x) = \bar{n}\exp(-q\psi(x)/T) \qquad \text{(A4)}$$

(The choice of the preexponential factor in eq A4 corresponds to the assumption of rapid decay of counterion

density outside the layer and to the condition $\psi(-H) = 0$.)

After linearization of eq A4 and taking into account eq A1, the set of Poisson–Boltzmann equations (A2)–(A4) reduced to the following equation for $\psi(x)$:

$$d^2\psi(x)/dx^2 - \kappa^2\psi(x) = 0, \quad -H \le x \le 0 \quad \text{(A5.1)}$$

$$d^2\psi(x)/dx^2 - \kappa^2\psi(x) = -4\pi\bar{n}q/\epsilon, \quad x \ge 0 \quad \text{(A5.2)}$$

The solution of eq A5 satisfying the boundary conditions

$$d\psi(x)/dx\Big|_{\substack{x=-H \\ x=\infty}} = 0 \quad \text{(A6)}$$

and the conditions of continuity for $\psi(x)$ and $\psi'(x)$ at $x = 0$ have at $H \gg \kappa^{-1}$ the following form:

$$\psi(x)/T \cong \frac{1}{2q}\exp(\kappa x), \quad -H \le x \le 0 \quad \text{(A7.1)}$$

$$\psi(x)/T \cong -\frac{1}{2q}\exp(-\kappa x) + 1/q, \quad x \ge 0 \quad \text{(A7.2)}$$

The corresponding profile of counterion density is given by

$$n(x) \cong \bar{n}(1 - \exp(\kappa x)/2), \quad -H \le x \le 0 \quad \text{(A8.1)}$$

$$n(x) \cong \bar{n}\exp(-\kappa x)/2, \quad x \ge 0 \quad \text{(A8.2)}$$

We see from eqs A7 and A8 that the counterion concentration decreases from a value equal to the mean concentration n in the depth of the layer to a zero level in a narrow range of $-r_D \le x \le r_D$ near the upper boundary of the layer ($x = 0$). The electrostatic field, $d\psi(x)/dx$, in the layer also differs from zero only in the range $-r_D \le x \le 0$ near the layer upper boundary.

Using eq A7 we can calculate the mean electrostatic force acting on an immobilized charge (stretching electrostatic force) as

$$f/T = -\int_{-H}^{0} \rho_{im}[d\psi(x)/dx]/T\,dx \cong -\rho_{im}/(2q) = \bar{n}/2 \quad \text{(A9)}$$

As follows from eq A9, the stretching electrostatic force (per unit area) applied to immobilized charges under the condition $\lambda \ll H$ really coincides with the accuracy of the numerical coefficient with the osmotic pressure of the gas of counterions inside the layer that justifies eq 20. Note that this electrostatic force is independent of the counterion charge q and any other electrostatic interaction parameters.

Salt-Added Solution. Let us consider the situation when a low molecular weight salt is added to the solution. The concentration of salt in the bulk of the solution is supposed to be equal to $\bar{n}_s$, and the charges of co- and counterions of salt are equal to q_s and $-q_s$, respectively. The total charge density in Poisson equation (A2), now includes the contributions of the immobilized charge, its own counterions, the co- and counterions of the salt. Assuming that all mobile ions are distributed in the solution according to the Boltzmann law, eq A4, we have the Poisson–Boltzmann equation for $\psi(x)$ in the following form:

$$d^2\psi(x)/dx^2 = (-4\pi/\epsilon)\rho_{im} + q\bar{n}\exp(-q\psi(x)/T) - 2\bar{n}_s\sinh(q_s\psi(x)/T), \quad -H \le x \le 0 \quad \text{(A10.1)}$$

$$d^2\psi(x)/dx^2 = (-4\pi/\epsilon)q\bar{n}\exp(-q\psi(x)/T) - 2\bar{n}_s\sinh(q_s\psi(x)/T), \quad x \ge 0 \quad \text{(A10.2)}$$

After linearization of this equation, we return to eq A5 in which, however, the inverse screening length κ defined by eq A1 should be substituted by κ_s, defined as

$$\kappa_s^2 = r_{Ds}^{-2} = 4\pi(q^2\bar{n} + 2q_s^2\bar{n}_s)/(\epsilon T) \cong 8\pi q_s^2\bar{n}_s/(\epsilon T) \quad \text{(A11)}$$

because now all mobile ions take part in the sceening of electrostatic interactions. The latter equality in eq A11 refers to the conditions of salt dominance, $q_s^2 n_s \gg q^2\bar{n}$, when the screening effect is determined primarily by salt ions.

Using the same boundary conditions (eq A6), we obtain the continuous and smooth at $x = 0$ solution of the linearized Poisson–Boltzmann equation in the salt-added case in the following form:

$$\psi(x)/T \cong \frac{1}{2q}(\kappa/\kappa_s)^2\exp(\kappa_s x), \quad -H \le x \le 0 \quad \text{(A12.1)}$$

$$\psi(x)/T \cong -\frac{1}{2q}(\kappa/\kappa_s)^2\exp(-\kappa_s x) + (1/q)(\kappa/\kappa_s)^2, \quad x \ge 0 \quad \text{(A12.2)}$$

Equation A12 shows that in the salt-added solution the width of the depletion zone for counterion density near the upper boundary of the layer and the depth of penetration of the electrostatic field into the layer depend on the salt concentration via κ_s (eq A11).

The mean electrostatic force (per unit area) applied to immobilized charge and calculated with the aid of eqs A9 and A12 is given by

$$f/T = [-\rho_{im}(2q)](\kappa/\kappa_s)^2 = (\bar{n}/2)(\kappa/\kappa_s)^2 \sim (\bar{n}^2/\bar{n}_s)(q/q_s)^2 \quad \text{(A13)}$$

We see that the $\bar{n}_s \gg \bar{n}$ and $q = q_s = 1$ this expression coincides with eq 26 for the stretching electrostatic force under the conditions of salt dominance.

References and Notes

(1) Alexander, S. *J. Phys.* **1977**, *38*, 983.
(2) de Gennes, P.-G. *Macromolecules* **1980**, *13*, 1069.
(3) Birshtein, T. M.; Zhulina, E. B. *Polym. Sci. USSR (Engl. Transl.)* **1983**, *25*, 2165.
(4) Zhulina, E. B. *Polym. Sci. USSR (Engl. Transl.)* **1984**, *26*, 885.
(5) Birshtein, T. M.; Zhulina, E. B. *Polymer* **1984**, *25*, 1453.
(6) Borisov, O. V.; Zhulina, E. B.; Birshtein, T. M. *Polym. Sci. USSR (Engl. Transl.)* **1988**, *30*, 772.
(7) Auroy, P.; Auvray, L.; Leger, L. *J. Phys.: Condens. Matter* **1992**, *2*, SA317.
(8) Auroy, P.; Auvray, L.; Leger, L. *Phys. Rev. Lett.* **1991**, *66*, 719.
(9) Auroy, P.; Auvray, L.; Leger, L. *Macromolecules* **1991**, *24*, 2523.
(10) Pryamitsyn, V. A.; Borisov, O. V.; Zhulina, E. B.; Birshtein, T. M. In *Modern Problems of Physical Chemistry of Solutions*; Donish-Leningrad University: Leningrad-Duschanbe, 1987; p 62. Zhulina, E. B.; Pryamitsyn, V. A.; Borisov, O. V. *Polym. Sci. USSR (Engl. Transl.)* **1989**, *31*, 205.
(11) Skvortsov, A. M.; Gorbunov, A. A.; Pavlushkov, I. V.; Zhulina, E. B.; Borisov, O. V.; Pryamitsyn, V. A. *Polym. Sci. USSR (Engl. Transl.)* **1988**, *30*, 1706.
(12) Zhulina, E. B.; Borisov, O. V.; Pryamitsyn, V. A. *J. Colloid Interface Sci.* **1990**, *137*, 495.
(13) Zhulina, E. B.; Borisov, O. V.; Pryamitsyn, V. A., Birshtein, T. M. *Macromolecules* **1991**, *24*, 140.
(14) Milner, S. T.; Witten, T. A.; Cates, M. E. *Europhys. Lett.* **1988**, *5*, 413.
(15) Milner, S. T. *Europhys. Lett.* **1988**, *7*, 695.
(16) Milner, S. T.; Witten, T. A.; Cates, M. E. *Macromolecules* **1988**, *21*, 2610.
(17) Pincus, P. *Macromolecules* **1991**, *24*, 2912. Ross, R.; Pincus, P. *Macromolecules* **1992**, *25*, 1503.
(18) Borisov, O. V.; Birshtein, T. M.; Zhulina, E. B. *J. Phys. II* **1991**, *1*, 521.
(19) Zhulina, E. B.; Borisov, O. V.; Birshtein, T. M. *J. Phys. II* **1992**, *2*, 63.
(20) Miklavic, S. J.; Marcelja, S. *J. Phys. Chem.* **1988**, *92*, 6718.

(21) Misra, S.; Varanasi, S.; Varanasi, P. P. *Macromolecules* **1989**, *22*, 4173.
(22) Odijk, T. *J. Polym. Sci., Polym. Phys. Ed.* **1977**, *15*, 447. Skolnick, J.; Fixman, M. *Macromolecules* **1977**, *12*, 688.
(23) Pincus, P. *Macromolecules* **1976**, *9*, 386.
(24) de Gennes, P.-G.; Pincus, P.; Velasco, R. M.; Brochard, F. *J. Phys.* **1976**, *37*, 1461.
(25) Khokhlov, A. R.; Khachaturian, K. A. *Polymer* **1982**, *23*, 1742.
(26) de Gennes, P.-G. *Scaling Concepts in Polymer Physics*; Cornell University Press: Ithaca, NY, 1985.
(27) Israelachvili, J. N. *Intermolecular and Surface Forces*; Academic Press: London, 1985.
(28) Barrat, J.-L.; Joanny, J.-F. *Europhys. Lett.* **1993**, *24*, 333.
(29) Wittmer, J.; Joanny, J.-F. *Macromolecules* **1993**, *26*, 2691.
(30) Auvray, L.; Auroy, P., private communication.
(31) Argillier, J. F.; Tirrell, M., preprint.
(32) Watanabe, H.; Patel, S.; Argiller, J. F.; Parsonage, E. E.; Mays, J.; Dan, N.; Tirrell, M. *Mater. Res. Soc. Symp. Proc.* **1992**, *249*, 255.